Supplement: Local-Scale Inversion of Agricultural Ammonia Emissions: A Case Study on Schiermonnikoog, the Netherlands

Simeng Li[1], **Enrico Dammers**[1,2], **Arjo Segers**[2], **and Jan Willem Erisman**[1]

[1]Institute of Environmental Sciences, Universiteit Leiden, Leiden, the Netherlands
[2]Air Quality and Emissions Research, Netherlands Organisation for Applied Scientific Research (TNO), Utrecht, 3584 CB, The Netherlands

Table S1. Agricultural emission, sector id 6

Enteric fermentation	Cattle	
	Sheep	
	Swine	
	Other animals	
Manure management	Cattle	dairy
		non-dairy
	Sheep	
	Swine	
	Buffalo	
	Goats	
	Horses	
	Mules and asses	
	Poultry	
	Broilers	
	Turkeys	
	Other poultry	
	Other animals	
Inorganic N-fertilizers (includes also urea application)		
Animal manure applied to soils		
Sewage sludge applied to soils		
Other organic fertilisers applied to soils (including compost)		
Urine and dung deposited by grazing animals		
Crop residues applied to soils		
Farm-level agricultural operations including storage, handling a		
Off-farm storage, handling and transport of bulk agricultural pr		
Cultivated crops		
Use of pesticides		
Rice cultivation		
Field burning of agricultural residues		
Urea application		
Other		

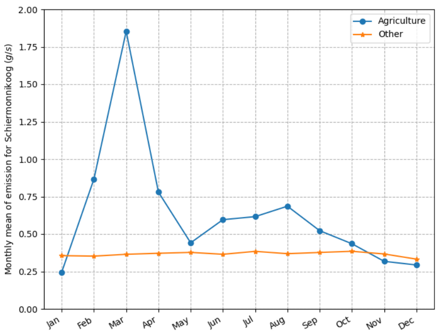

(a) Emission in 2019

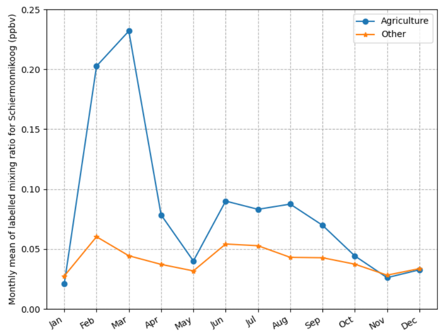

(b) Concentration in 2019

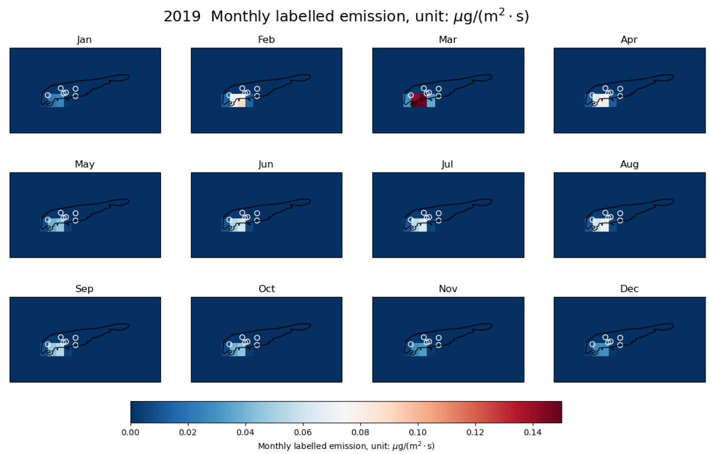

(c) Schier_agri Emission in 2019

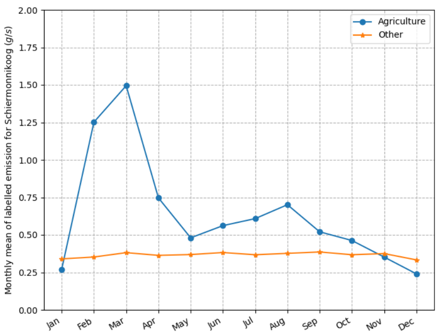

(d) Emission in 2022

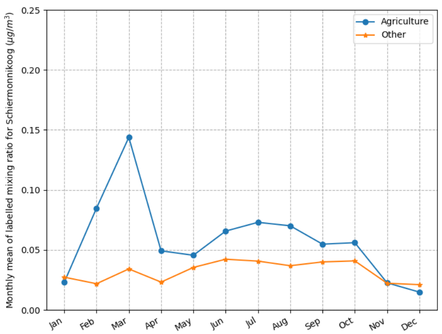

(e) Concentration in 2022

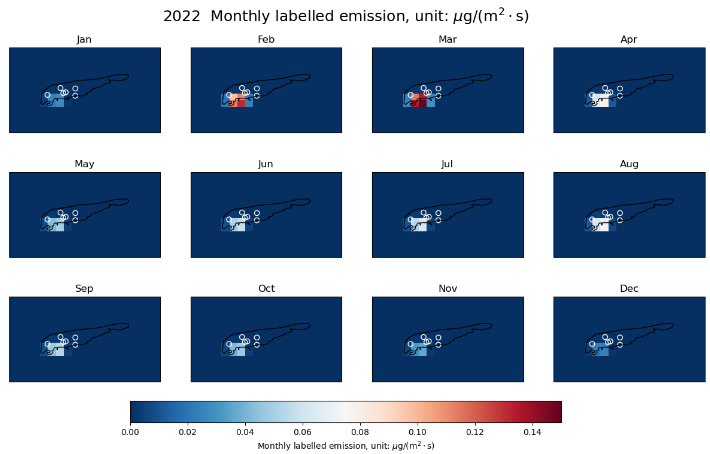

(f) Schier_agri Emission in 2022

Figure S1. The monthly time profile for prior emissions and their contribution to local ammonia concentration on Schiermonnikoog in 2019 and 2022.

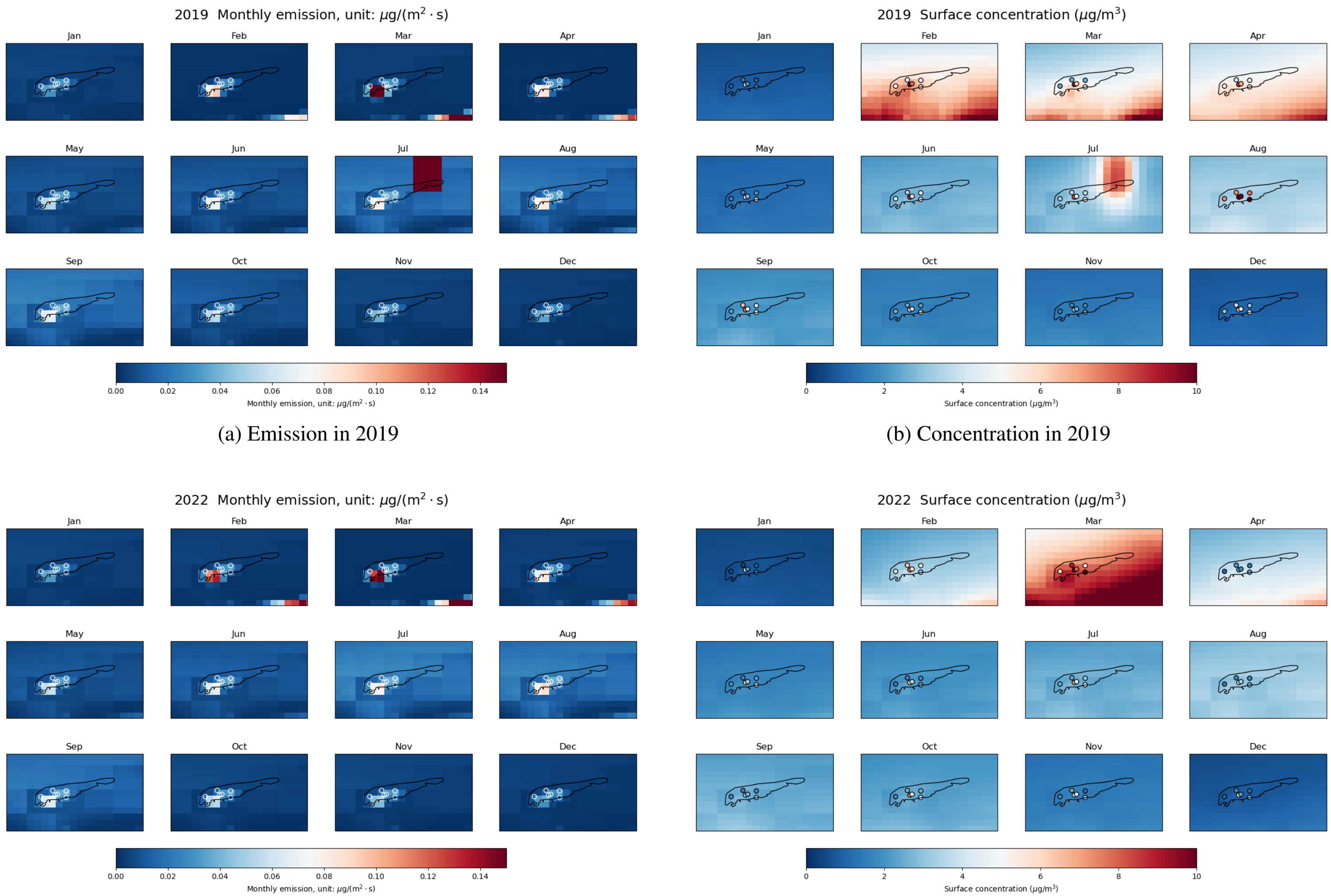

(a) Emission in 2019

(b) Concentration in 2019

(c) Emission in 2022

(d) Concentration in 2022

Figure S2. The monthly time profile for prior emissions and their contribution to local ammonia concentration on Schiermonnikoog in 2019 and 2022.

If we increase the measurements at the same sites, and then average those into one "superobservation" for that site, the total error could be reduced significantly and might be comparable to relatively high-quality measurement data. Assuming we have 6 sets of available MAN data at the very same site, then the total error should be, derived from Noordijk et al. (2020) Sect. 3.3:

$$s_{0\text{ tot}} = \left(\frac{s^2_{0\text{ MAN measuremnt}} + s^2_{0\text{ cal method}}}{6} \right)^{\frac{1}{2}} \approx 0.36\mu\text{g/m}^3 \tag{1}$$

$$\text{RSD}_{\text{tot}} = \left[\text{RSD}^2_{\text{MAN measuremnt}} + \frac{\text{RSD}^2_{\text{cal method}} + \text{RSD}^2_{\text{cal standard}}}{6} \right]^{\frac{1}{2}} \approx 10\% \tag{2}$$

While enhancing a single MAN site alone does not achieve the same performance as adding a single LML-like site (see Fig. S3a), substituting all six MAN sites on Schiermonnikoog with corresponding superobservations yields substantial improvements (Fig. S3b). In fact, this approach performs even better than the LML-like configuration in March and April. More details are provided in the Supplement.

References

Noordijk, H., Braam, M., Rutledge-Jonker, S., Hoogerbrugge, R., Stolk, A., and van Pul, W.: Performance of the MAN ammonia monitoring network in the Netherlands, Atmospheric Environment, 228, 117 400, https://doi.org/https://doi.org/10.1016/j.atmosenv.2020.117400, 2020.

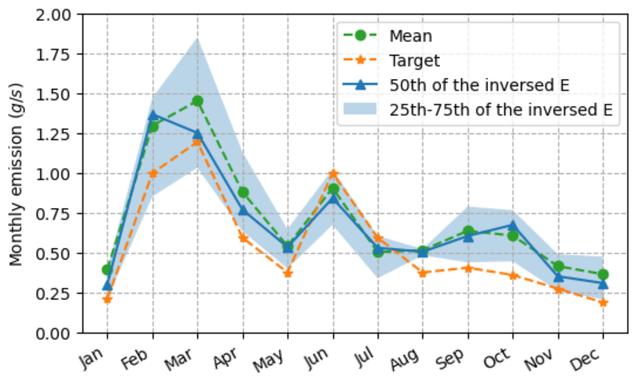

(a) One superobservation at Schiermonnikoog-Kooiduinen

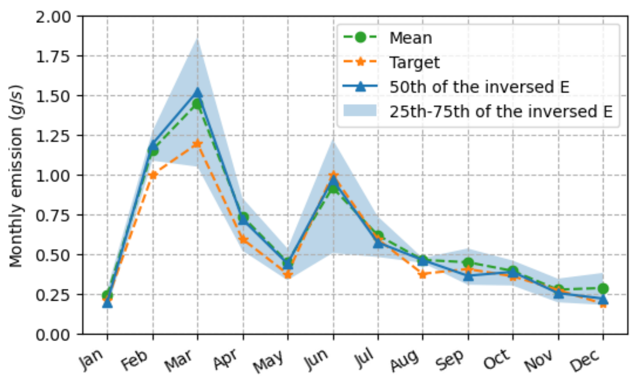

(b) Substitute all the 6 sites with superobservations

Figure S3. Posterior emission of the inversion with superobservations

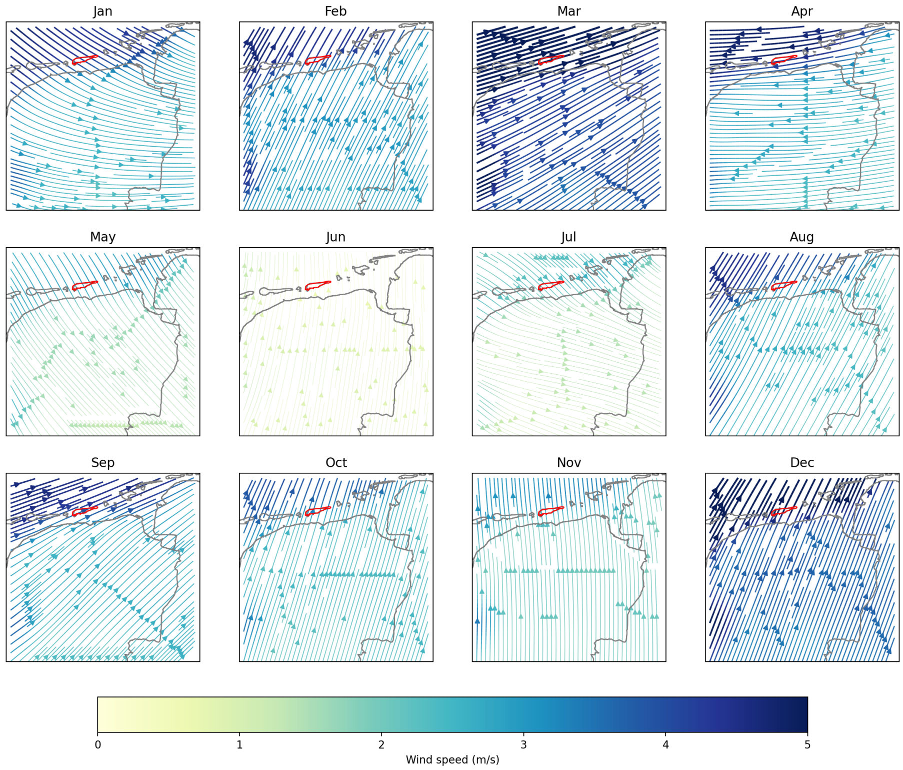

(a) 2019

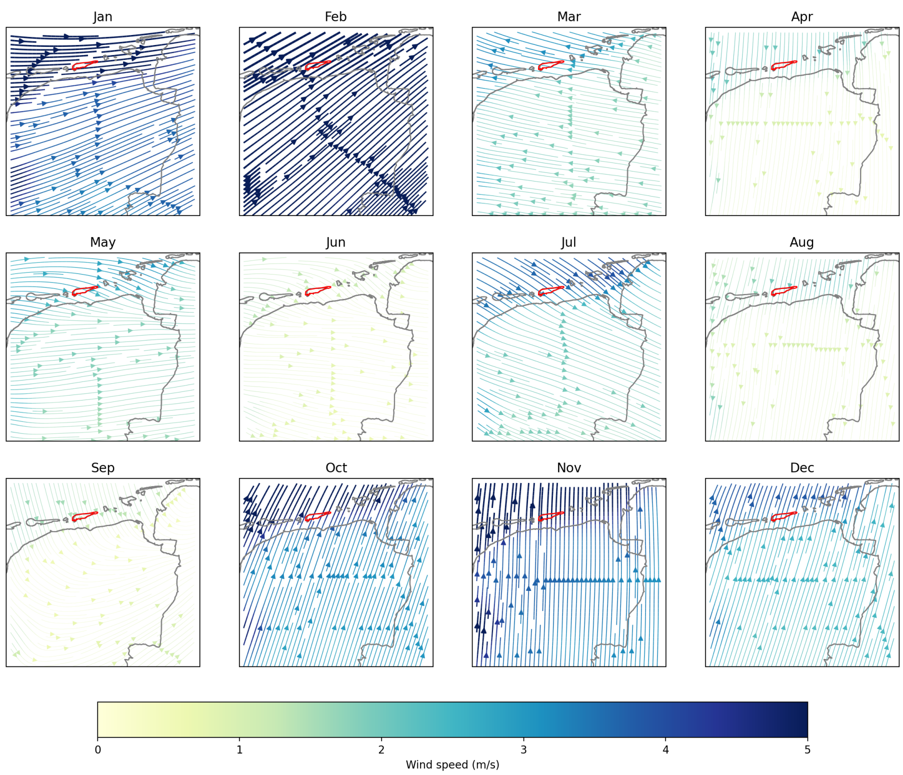

(b) 2022

Figure S4. Maps of wind field for 2019 (a) and 2022 (b).